Int. J. Morphol.,
44(1):92-98, 2026.

Target Localization for Botulinum Neurotoxin Type A Injection in the Treatment of Pediatric Muscular Torticollis

Localización del Objetivo para la Inyección de Neurotoxina Botulínica Tipo A en el Tratamiento de la Tortícolis Muscular Pediátrica

Ren Chen[1]; Hong Chen[1];Jun Zhao[1] & Shengbo Yang[2]

CHEN, R.; CHEN, H.; ZHAO, J. & YANG, S. Target localization for botulinum neurotoxin type A injection in the treatment of pediatric muscular torticollis. *Int. J. Morphol., 44(1)*:92-98, 2026.

SUMMARY: This study aims to examine the intramuscular nerve distribution pattern of the sternocleidomastoid muscle (SCM) in children and to identify the center of the intramuscular nerve-dense region (CINDR), offering morphological guidance for Botulinum neurotoxin type A (BoNT-A) injections in the treatment of pediatric muscular torticollis. A total of 24 Chinese pediatric cadaveric specimens were analyzed. The intramuscular nerve distribution of the SCM was visualized using a modified Sihler's staining technique. Spiral computed tomography was employed to determine the surface puncture location and depth of the CINDR. A percutaneous longitudinal reference line was defined from the lowest point of the jugular notch of sternum to the chin tip of the mandible, and a transverse reference line was established from the lowest point of the jugular notch of sternum to the acromion. A band-shaped, intramuscular nerve-dense region was identified in the middle portion of the SCM, oriented obliquely from superoposterior to inferoanterior. The CINDR projected at (38.29 ± 1.39)% along the transverse reference line and at (68.62 ± 1.46)% along the longitudinal reference line. The puncture depth of the CINDR was measured as 10.18 ± 1.68 mm. Defining the surface location and depth of the CINDR in the pediatric SCM aids in precise target localization and enhances the efficacy of BoNT-A injections for treating pediatric muscular torticollis.

KEY WORDS: Pediatric muscular torticollis; Sternocleidomastoid muscle; Innervation; Botulinum neurotoxin type A; Neuromuscular blockade.

INTRODUCTION

The etiology of pediatric torticollis is multifactorial and encompasses several types: (1) congenital muscular torticollis, caused by intrauterine compression, malposition, birth trauma, or congenital developmental abnormalities; (2) congenital osseous torticollis, resulting from cervical vertebral malformations; (3) postural/habitual torticollis; (4) ocular torticollis, which compensates for diplopia; (5) infectious or inflammatory torticollis, due to deep cervical tissue infection or inflammation; (6) neurogenic torticollis, associated with cerebral palsy or intracranial tumors; and (7) traumatic torticollis of the neck (El Mandour *et al*., 2021). Despite their differences, these conditions share common features, such as head tilt and restricted cervical mobility. Among them, muscular torticollis accounts for more than 50 % of pediatric torticollis cases (Garikipati & Gibb, 2013). Current clinical management strategies include orthotic correction, massage therapy, surgical intervention, and the injection of Botulinum neurotoxin type A (BoNT-A) (Jiang *et al*., 2018; Kaplan *et al*., 2018). BoNT-A injection has been widely adopted in clinical practice due to its non-invasiveness, reversibility, and high patient compliance (Sargent *et al*., 2019).

Injection of BoNT-A into the sternocleidomastoid muscle (SCM) inhibits the release of acetylcholine at the presynaptic membrane, inducing chemical denervation of the SCM and resulting in muscle relaxation. Furthermore, by suppressing fibroblast differentiation and proliferation, BoNT-A can reverse the fibrotic progression of the SCM, thereby alleviating craniofacial deviation caused by abnormal muscle traction (Joseph *et al*., 2023; Mitchell *et al*., 2023). Current SCM-targeting strategies for BoNT-A injection include administering 30 units of BoNT-A at 3–4 points along the

[1] Department of Pediatric Internal Medicine, Maternal and Child-Care Hospital of Zunyi, People's Republic of China.
[2] Department of Anatomy, Zunyi Medical University, Zunyi, People's Republic of China.
FUNDING. This work was supported by the National Natural Science Foundation of China [grant number 32260217]; Science and Technology Project of Zunyi [grant number HZ-2023-364]. The funding agencies had no role in study design, data collection, and analysis, decision to publish, or preparation of the manuscript.

Received: 2025-09-21 Accepted: 2025-11-21

longitudinal axis of the SCM or performing a single-point injection into the muscle beneath the external jugular vein. These methods, whether using high-dose single-point or multi-point injections, fail to precisely target effective intramuscular regions, which may lead to complications such as muscle fibrosis, antibody formation, and inconsistent therapeutic outcomes.

The site of action of BoNT-A is the neuromuscular junction, specifically within the motor endplate zone (Lehoux *et al*., 2020). The therapeutic efficacy of BoNT-A is closely related to the proximity of the injection site to the motor endplates; a deviation of 5 mm from the motor endplate can reduce the therapeutic effect by approximately 50 % (Yu *et al*., 2023). However, staining of human motor endplate zones is limited by the need for fresh specimens collected within 3 h *postmortem*. Previous studies have indicated that the intramuscular nerve dense region (INDR) corresponds to the location of the motor endplate zone, and that the center of the intramuscular nerve dense region (CINDR) can serve as a surrogate target for BoNT-A injection (Wang *et al*., 2024). This study aims to visualize the INDR in the pediatric sternocleidomastoid muscle using a modified Sihler's staining method and subsequently employ spiral computed tomography CT scanning to determine the surface puncture percentage, position, and depth of the CINDR, providing morphological guidance to optimize target localization and improve the therapeutic efficacy of BoNT-A injections in pediatric muscular torticollis.

MATERIAL AND METHOD

Specimens and Ethics. A total of 24 Chinese pediatric cadaveric specimens (12 males, 12 females), aged 3–16 years (mean ± SD: 8.13 ± 3.47 years), with no history of neuromuscular disorders or head and neck malformations, were collected. Of these, 12 specimens (equal numbers of males and females) were fixed in formalin for Sihler's staining, while the remaining 12 were preserved by freezing to avoid tissue distortion caused by formalin fixation, allowing for target localization. Informed consent for the use of the specimens was obtained from their legal guardians and immediate family members. The study was conducted in strict accordance with the Declaration of Helsinki (1964) and its subsequent amendments and was approved by the Ethics Committee of Zunyi Medical University (#2022-1-008).

Gross Anatomical Observation and Reference Line Design. The cadavers were positioned supine. A midline incision was made from the menton extending inferiorly to the manubrium of the sternum, followed by a transverse incision extending laterally along the inferior margin of the mandible to the mastoid process. An additional transverse incision was made from the lowest point of the jugular notch of sternum, extending laterally along the inferior margin of the clavicle to the acromion. The skin, subcutaneous tissue, and platysma were reflected laterally as a single layer, ensuring close contact with the surface of the SCM. The SCM was fully exposed to assess its gross morphology, fiber orientation, origin and insertion points, nerve supply, and sites of intramuscular nerve entry, while also noting whether blood vessels accompanied the nerve entry points. To clarify the superior-inferior and medial-lateral relationships between the BoNT-A injection targets within the SCM and bony landmarks, a longitudinal reference line (L-line) was designed as the curve connecting the lowest point of the jugular notch of sternum (point a) to the chin tip of the mandible (point b). The horizontal reference line (H-line) was defined as the curve connecting point a, to the acromion (point c).

Determination of the Center of Intramuscular Nerve-Dense Region Using Modified Sihler's Staining. The bilateral SCMs were carefully dissected from 12 formalin-fixed cadaveric specimens. A modified Sihler's staining protocol was used to visualize the intramuscular nerve distribution (Zhou *et al*., 2023), consisting of six sequential steps: depigmentation, decalcification, staining, destaining, neutralization, and clearing. Once the intramuscular nerve branches and dense regions were clearly visualized, images were captured using an X-ray viewing box and archived. In Adobe Photoshop 2020 (Adobe Systems Inc., USA), the INDR was outlined following the principle of "less rather than more." After selecting the INDR boundary, the geometric center was determined using the Control+T function and defined as the CINDR. Using a calibrated scale, the percentage positions of the INDR and CINDR along the muscle's longitudinal and transverse axes were measured, and the area of the INDR was also quantified.

Spiral Computed Tomography (CT) Localization of the CINDR. The 12 fresh-frozen cadaveric specimens were thawed, and the SCM was dissected and fully exposed. Based on the percentage positions of the CINDR along the muscle's length and width obtained from Sihler's staining, a mixture of medical barium sulfate powder (Shandong Jiashuo Radiation Protection Engineering Co., China) and 801 glue(Wenzhou 801 Glue Co., China) was prepared and injected into the SCM to mark the CINDR. Subsequently, a puncture needle was inserted into the CINDR along the simulated injection trajectory, and the tissue layers were sutured sequentially. At surface landmarks a (the lowest point of the jugular notch of sternum), b (chip tip), and c (acromion), needles were inserted, and barium-soaked threads were sutured between points a–b and b–c to represent the longitudinal reference line (L-line) and horizontal reference line (H-line), respectively. Spiral computed

tomography (64-slice, Siemens, Germany) was performed for scanning and three-dimensional reconstruction. Scanning parameters were set as follows: 120 kV, 1mm slice thickness, collimation 64 × 0.75 mm, and pitch 1:1. The surface projection of the CINDR was defined as point P. Within the Syngo system (Siemens, Germany), the curve measurement tool was used to measure the total lengths of the two reference lines along the skin surface (H for the total length of the horizontal reference line and L for the total length of the longitudinal reference line). A perpendicular line was drawn from point P to intersect the H-line, with the intersection defined as point PH. A horizontal line parallel to the H-line passing through point P intersected the L-line at point PL. The distance from point a to P_H was recorded as H´, and the distance from point a to P_L was recorded as L´. The percentage positions of point P along the surface were calculated as H´/H × 100 % and L´/L × 100 %. The depth of perpendicular puncture from point P to the CINDR was measured using the straight-line measurement tool.

Statistical Analysis. Data analysis was conducted using SPSS version 29.0 software (IBM Corporation, Armonk, NY, USA). All measurements were expressed as a percentage of individual reference lines ($x \pm s$, %) to eliminate the influence of inter-individual variability. As the data conformed to a normal distribution, comparisons between the left and right sides were performed using paired t-tests, while comparisons between male and female specimens were performed using independent-samples t-tests. $P < 0.05$ was considered statistically significant.

RESULTS

Gross Anatomical Observations. The SCM exhibited a long, strap-like morphology. Its origins were located at the anterior surface of the manubrium (sternal head) and the medial one-third of the clavicle (clavicular head). The muscle fibers ascended and converged at the middle portion of the muscle, inserting onto the lateral surface of the mastoid process and the lateral one-third of the occipital bone. The mid-belly of the SCM was further subdivided into the sternal head portion, superficial clavicular head portion, and deep clavicular head portion. The accessory nerve entered the muscle on its deep surface at approximately the upper one-third to one-fourth of the muscle's length. Among the 24 sides examined, 17 sides showed nerve entry posterior to the clavicular head, while 7 sides exhibited nerve entry through the clavicular head. The superficial surface of the SCM was covered by skin, cervical fascia, and the platysma muscle, and lay adjacent to the great auricular nerve and transverse cervical nerve. Its deep surface was in close proximity to major neurovascular structures, including the internal jugular vein, common carotid artery, and the vagus nerve. Medially, the SCM was bordered by the sternohyoid and sternothyroid muscles, whereas laterally, it, along with the trapezius muscle, formed the posterior triangle of the neck.

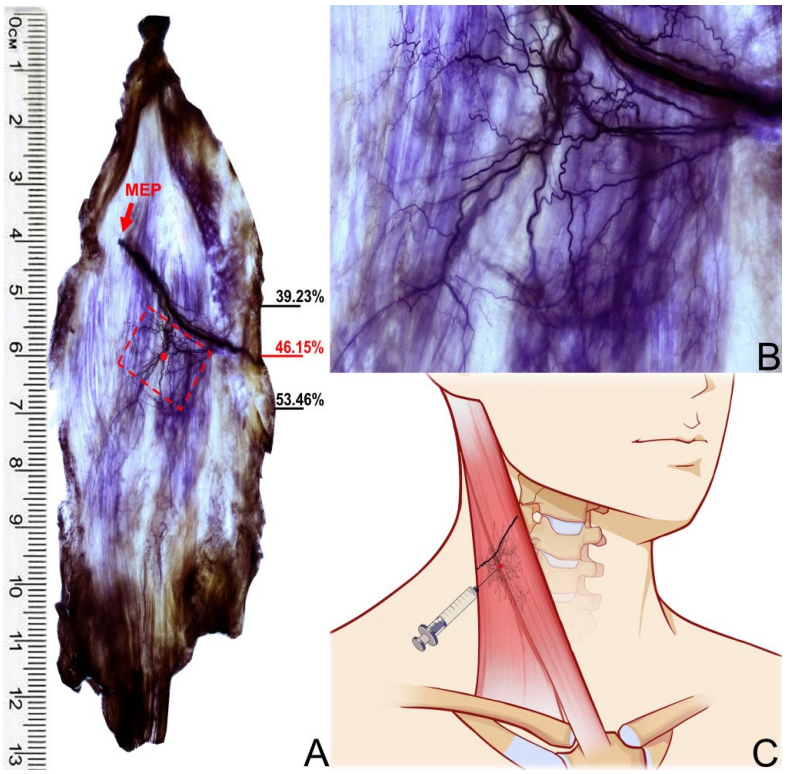

Fig. 1. Sihler's Staining of Intramuscular Nerves in the Sternocleidomastoid Muscle: A: Sihler's staining demonstrating the intramuscular nerve distribution pattern. The red box indicates the location of the INDR, the red dot represents the CINDR, and the red arrow points to the nerve entry site. B: Detailed view of the intramuscular nerve distribution within the red box in panel A. C: Schematic illustration of BoNT-A injection into the CINDR of SCM, with the red dot indicating the CINDR.

Sihler's Staining of the Sternocleidomastoid Muscle. After entering the upper-middle portion of the muscle at its deep surface, the accessory nerve coursed obliquely from superoposterior to inferoanterior. Branches arising from the lower part of the main nerve trunk were more numerous than those originating from the upper part. Small nerve branches surrounding the main trunk anastomosed with each other in the mid-belly region of the muscle, spanning (38.97 ± 1.62)% to (56.95 ± 2.03)% along the muscle's longitudinal axis, forming a band-shaped INDR oriented obliquely from superoposterior to inferoanterior (Fig.1). The area of the INDR was (1.89 ± 0.13) cm^2. The center of the CINDR was located at (45.79 ± 2.03) % along the muscle's length and (53.86 ± 1.61)% along the muscle's

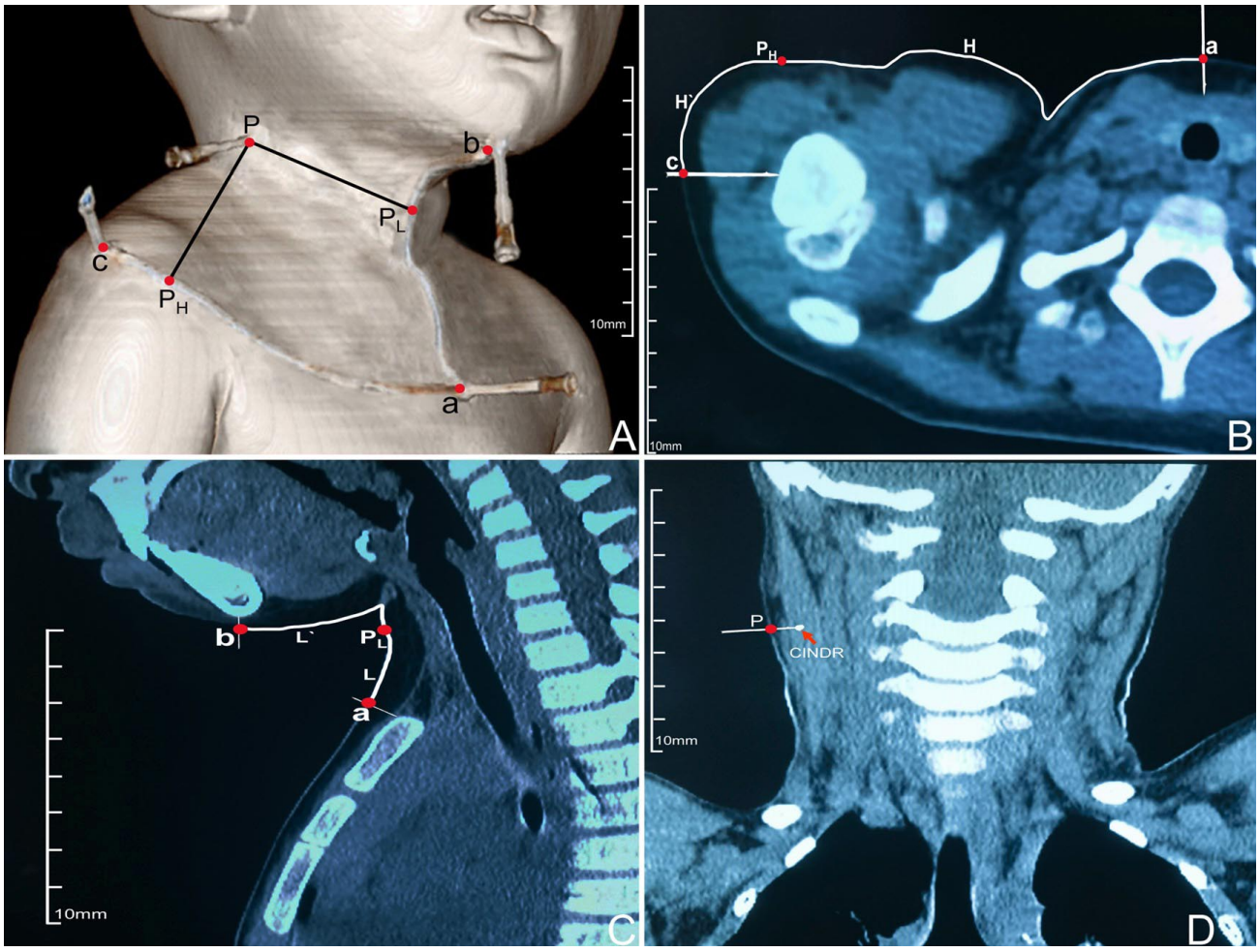

Fig. 2. Spiral CT Localization of the Intramuscular Nerve Dense Region Center (CINDR) in the Male Sternocleidomastoid Muscle: A: Three-dimensional spiral CT reconstruction showing the surface projection of the CINDR and the constructed reference lines. a = the lowest point of the jugular notch of sternum, b = chin tip of the mandible, c = the acromion, P = the projection of the CINDR on the body surface. PH denotes the intersection of the perpendicular line from P with the H-line, and PL denotes the intersection of the perpendicular line from P with the L-line. ca = total length of H-line, a–PH = H', ab = total length of L-line, a–PL = L'. B: Measurement of the lengths of H-line and H' on the transverse section. C: Measurement of the lengths of L-line and L' on the sagittal section. D: Measurement of the depth of the CINDR on the coronal section.

width. Comparisons between left and right sides, as well as between male and female specimens, showed no statistically significant differences ($P > 0.05$).

Spiral CT Localization of the CINDR in SCM. The surface projection of the CINDR (point P) of SCM was located inferior to the mandible, near the inferior angle. The corresponding percentage positions of this point along the horizontal reference line (H-line) and longitudinal reference line (L-line) are shown in Figure 2. Measurements showed that the projection point of the CINDR onto the transverse reference line (PH point) was located at 38.29 ± 1.39 % of its total length, while the projection point onto the longitudinal reference line (PL point) was at 68.62 ± 1.46 % of its total length. The perpendicular puncture depth from the skin at the P point was 10.18 ± 1.68 mm. Statistical analysis revealed no significant differences between the left and right sides or between sexes ($P > 0.05$) (Fig. 3).

DISCUSSION

Necessity and Significance of Target Localization for BoNT-A Injection in Pediatric Muscular Torticollis. This study is crucial because pediatric neck muscles are small, layered, and located near vital neurovascular structures, making traditional blind injections prone to complications. The pathological heterogeneity of the disease and the lack of precise standards for different lesion types in current clinical methods result in variable therapeutic outcomes. Therefore, further anatomical investigation is urgently needed

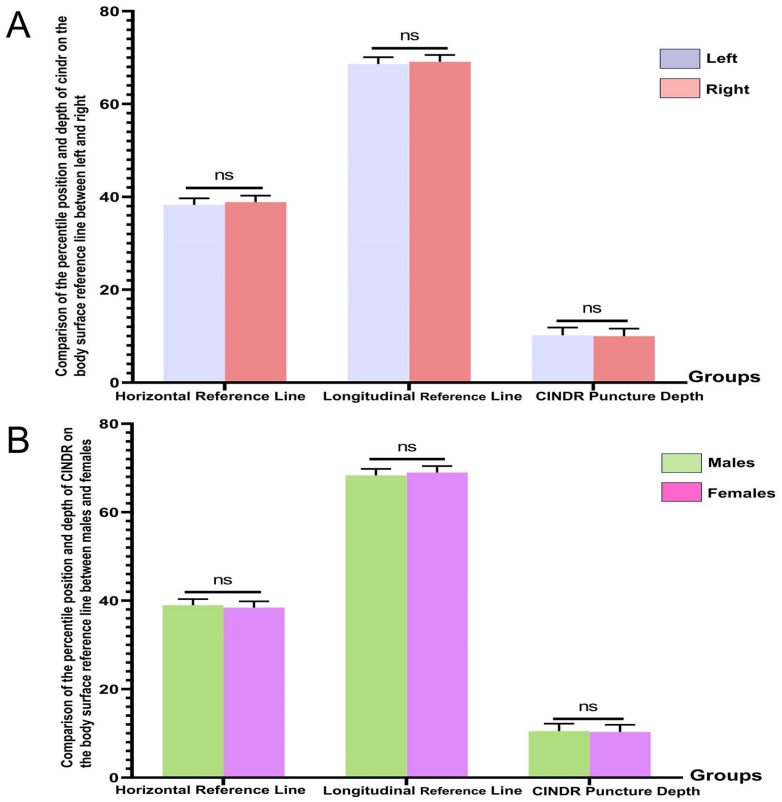

Fig.3. Percentage Positions and Puncture Depths of the CINDR of SCM Relative to Reference Lines: A: Comparison of the CINDR body surface percentage positions and perpendicular puncture depths between the left and right sides. B: Comparison of the CINDR percentage positions and puncture depths between male and female specimens. ns = $P > 0.05$ 2

to achieve technical advancements. Clinically, accurate target localization can greatly enhance therapeutic efficacy by delivering the drug directly to the contracted muscle fibers, while minimizing the risk of adverse effects such as dysphagia, which can result from drug diffusion, thereby enabling individualized treatment. Academically, this research contributes to a deeper understanding of disease mechanisms and supports the development of standardized, reproducible treatment protocols, advancing the field toward precision medicine. From a socioeconomic perspective, improving the success rate of a single treatment session reduces the need for repeated interventions or surgery, prevents secondary craniofacial deformities, improves the long-term quality of life and prognosis for affected children, and reduces overall healthcare costs. Consequently, this study marks a critical step in improving the treatment of pediatric torticollis while ensuring both safety and therapeutic effectiveness.

Anatomy of the Sternocleidomastoid Muscle and Selection of BoNT-A Injection Sites. The SCM originates from the sternum and clavicle, with the clavicular head arising from the medial one-third of the clavicle and the sternal head from the superior part of the manubrium. The two muscle bundles ascend and converge in the middle portion of the neck to form a single muscle mass, inserting onto the mastoid process. Although previous studies have reported anatomical variations, such as three-headed or multi-headed forms (Maneenin *et al*., 2023), the specimens in this study were all of the double-headed type after dissection. This discrepancy may be due to the small sample size. The great auricular nerve runs along the superficial surface of the superomedial portion of the SCM, while the transverse cervical nerve courses along the superficial surface of the mid-portion of the muscle. The external jugular vein courses superficially across the inferomedial portion of the SCM, running obliquely downward from the angle of the mandible toward the middle of the clavicle. Additionally, some muscular branches of the superior thyroid artery or occipital artery are distributed on the muscle surface. These neurovascular structures are at risk of injury during BoNT-A injections.

Based on anatomical findings, the superficial surface of the SCM contains the great auricular nerve, transverse cervical nerve, and the external jugular vein, among other neurovascular structures, which must be carefully avoided during BoNT-A injection. In traditional treatment protocols for pediatric muscular torticollis, 3–4 injection points along the long axis of the SCM are commonly selected. However, this approach carries a relatively high risk of nerve or vascular injury. Moreover, Sihler's staining of the INDR indicates that the muscle tissue beneath the external jugular vein contains very sparse terminal nerve branches, and injections at this site would markedly reduce therapeutic efficacy. Therefore, accurately identifying the optimal intramuscular BoNT-A injection target within the SCM and its anatomical relationships has significant clinical guidance value.

Challenges of Intramuscular BoNT-A Injection in the SCM. Intramuscular injection of BoNT-A into the SCM has become a widely accepted treatment for pediatric muscular torticollis due to its proven efficacy, minimal invasiveness, and high patient compliance (Qiu *et al*., 2020). Currently, clinical techniques for SCM BoNT-A injection are primarily categorized into single-point and multiple-point approaches. For example, 30 units of BoNT-A may be divided among 3–4 injection points along the long axis of the SCM, or a single injection may be administered within the SCM beneath the external jugular vein. In clinical

practice, single-point injections present challenges in precise dose control, while multiple-point injections, although allowing for better dose distribution, increase the number of punctures and the associated discomfort for the patient. Current injection techniques are largely designed to avoid injury to adjacent anatomical structures. Anatomical studies highlight that numerous neurovascular branches course along the superficial surface of the SCM, particularly the muscle branches originating from the thyroid and occipital arteries, with considerable inter-individual variation in their trajectories. Consequently, commonly used injection sites carry a risk of damaging critical nerves or vessels, potentially resulting in sensory disturbances or bleeding within the injection area, and may not represent the optimal choice. Although ultrasound-guided injection provides real-time imaging that clearly delineates the SCM contours and larger superficial neurovascular structures, thereby minimizing the risk of vascular or neural injury (Alheet *et al*., 2024), this technique cannot identify or localize the INDR.

Studies on Intramuscular Nerve Distribution in the SCM. Previous microscopic anatomical studies have shown that the nerve innervating the SCM enters the muscle approximately 5.2?± 1.8 cm below the mastoid process (Silawal *et al*., 2022). After entry, the main trunk courses obliquely downward, and its intramuscular trajectory can be classified into three types: Type A (non-penetrating), accounting for 45.9 %, in which the main trunk does not traverse the muscle; Type B (partially penetrating), comprising 50.8 %, where the trunk penetrates the medial surface of the SCM and subsequently re-emerges medially before projecting toward the trapezius; and Type C (fully penetrating), accounting for 3.3 %, in which the main trunk traverses completely from the medial to the lateral surface of the SCM, posing a risk of being misidentified as the great auricular nerve or transverse cervical nerve during clinical procedures, potentially resulting in nerve injury. Although previous methods have roughly delineated the intramuscular course of the nerves, they have inherent limitations. During dissection, small nerve branches are frequently disrupted and segments of muscle tissue are removed, making it difficult to accurately reflect the relationship between nerve branch distribution and muscle structure. Other studies using Sihler's staining have demonstrated that the SCM's INDR is located between the hyoid bone and cricoid cartilage, corresponding to approximately 30–60 % of the muscle length, which is largely consistent with the INDR range identified in the present study (Gülcan *et al*., 2024). However, the number of fine nerve branches visualized in those studies was considerably lower than in the present experiment, rendering it impossible to determine the precise location of the INDR through direct visualinspection, and no localization study of the INDR was conducted. In this study, by optimizing the reagent concentrations in the modified Sihler's staining protocol, a greater number of tertiary and quaternary nerve branches were clearly visualized, and spiral CT scanning enabled precise localization of the CINDR. Despite clearly demonstrating the distribution pattern of the INDR, the present study did not provide a three-dimensional representation of the anatomical relationship between superficial and deep intramuscular nerve branches.

Localization Study of the CINDR. Staining of human motor endplate bands requires fresh specimens within 3 h *postmortem*, which is difficult to obtain and limits the practical feasibility of motor endplate localization. Given that the INDR coincides with the location of the motor endplate band, several studies have proposed the CINDR as a surrogate target for BoNT-A injection (Hu *et al*., 2022 Wang *et al*., 2022 Hu *et al*., 2023). Recently, our team conducted experiments on the rabbit masseter muscle, demonstrating that BoNT-A injection at the CINDR resulted in superior therapeutic outcomes compared to injections at conventional sites (Chen *et al*., 2025). Therefore, precise localization of the CINDR in the pediatric SCM in this study is expected to improve targeting accuracy and enhance the therapeutic efficacy of BoNT-A injections in the management of pediatric muscular torticollis.

In summary, although previous studies have investigated the intramuscular nerve distribution of the adult SCM (Gülcan *et al*., 2024), the CINDR was not specifically localized. Even when adult CINDR data are available, they cannot serve as a substitute for pediatric localization results due to growth-related variations in body size. Therefore, the precise localization of CINDR in pediatric SCM, including its surface percentage position and puncture depth via spiral CT in this study, offers valuable clinical guidance. Nonetheless, this study has some limitations, including the absence of racial subgroup analysis, a relatively small sample size, and the lack of validation in clinical practice.

CONCLUSIONS

The CINDR of the Sternocleidomastoid Muscle can be served as an Ideal injection site for BoNT-A in pediatric muscular torticollis. This approach enhances the targeting accuracy and efficacy of BoNT-A injections.

ACKNOWLEDGMENTS. The authors would like to acknowledge Xufeng Tian for her excellent technical assistance in spiral CT scanning. The authors sincerely thank those who donated their bodies to science so that this anatomical research could be performed. Results from such research can potentially increase mankind's knowledge and improve patient care. Therefore, these donors and their families deserve our utmost gratitude.

CHEN, R.; CHEN, H.; ZHAO, J. & YANG, S. Localización del objetivo para la inyección de neurotoxina botulínica tipo A en el tratamiento de la tortícolis muscular pediátrica. *Int. J. Morphol., 44(1)*:92-98, 2026.

RESUMEN: Este estudio tuvo como objetivo examinar el patrón de distribución nerviosa intramuscular del músculo esternocleidomastoideo (MECM) en niños e identificar el centro de la región densa de nervios intramusculares (CRDNI), ofreciendo una guía morfológica para las inyecciones de neurotoxina botulínica tipo A (BoNT-A) en el tratamiento de la tortícolis muscular pediátrica. Se analizaron 24 muestras de cadáveres pediátricos chinos. La distribución nerviosa intramuscular del MECM se visualizó mediante una técnica de tinción de Sihler modificada. Se empleó una tomografía computarizada espiral para determinar la ubicación de la punción superficial y la profundidad de la CRDNI. Se definió una línea de referencia longitudinal percutánea desde el punto más bajo de la incisura supraesternal hasta el ápice del mentón mandibular, y se estableció una línea de referencia transversal desde el punto más bajo de la incisura supraesternal hasta el acromion. Se identificó una región intramuscular densa en forma de banda en la porción media del MECM, orientada oblicuamente de superoposterior a inferoanterior. El CRDNI se proyectó a 38,29 ± 1,39 % a lo largo de la línea de referencia transversal y a 68,62 ± 1,46 % a lo largo de la línea de referencia longitudinal. La profundidad de punción del CRDNI fue de 10,18 ± 1,68 mm. Definir la ubicación superficial y la profundidad del CRDNI en el MECM pediátrico facilita la localización precisa del objetivo y mejora la eficacia de las inyecciones de BoNT-A para el tratamiento de la tortícolis muscular pediátrica.

PALABRAS CLAVE: Tortícolis muscular pediátrica; Músculo esternocleidomastoideo; Inervación; Neurotoxina botulínica tipo A; Bloqueo neuromuscular.

REFERENCES

Alheet, G.; Barut, Ç. & Ögüt, E. Quantitative analysis of surgical landmarks of the face in fixed cadaveric heads: Clinical and anatomical implications. *Surg. Radiol. Anat., 46(11)*:1811-23, 2024.

Brin, J. F. & Burstein, R. Botox (onabotulinumtoxinA) mechanism of action. *Medicine, 102(S1)*:e32372, 2023.

Chen, R.; He, L.; He, X.; Jiang, X. & Yang, S. Experimental study of the center of the intramuscular nerve dense region of the masseter muscle as the optimal botulinum neurotoxin A injection site. *Ann. Anat., 261*:152697, 2025.

El Mandour, J.; Cherraqi, A.; Sahli, H.; El Haddad, S.; Allali, N. & Chat, L. Torticollis imaging in pediatric settings. *J. Neuroradiol., 48(4)*:216-7, 2021.

Garikipati, V. & Gibb, W. R. Congenital muscular torticollis and cervical dystonia. *J. Neurol. Neurosurg. Psychiatry, 84(11)*:e2, 2013.

Gülcan, M.; Çelik, S.; Tomruk, C.; Bilge, O. & Uyanıkgil, Y. Intramuscular nerve distribution of the sternocleidomastoid muscle for botulinum toxin injection. *Surg. Radiol. Anat., 46(6)*:905-13, 2024.

Hu, X.; Hu, S.; Wang, M.; Xiong, W. & Yang, S. Localization of the nerves innervating the pelvic floor muscles: An application to pelvic pain treatment. *Clin. Anat., 35(7)*:979-86, 2022.

Hu, X.; Wang, M.; He, X.; Chen, P.; Jia, F.; Wang, D. & Yang, S. Division of neuromuscular compartments and localization of the center of the intramuscular nerve dense region in pelvic wall muscles based on Sihler's staining. *Anat. Sci. Int., 99(1)*:127-37, 2023.

Jankovic, J.; Tsui, J. & Brin, M. F. Treatment of cervical dystonia with botox (onabotulinumtoxinA): Development, insights, and impact. *Medicine, 102(S1)*:e32403, 2023.

Jiang, B.; Zu, W.; Xu, J.; Xiong, Z.; Zhang, Y.; Gao, S.; Ge, S. & Zhang, L. Botulinum toxin type A relieves sternocleidomastoid muscle fibrosis in congenital muscular torticollis. *Int. J. Biol. Macromol., 112*:1014-20, 2018.

Kaplan, S. L.; Coulter, C. & Sargent, B. Physical therapy management of congenital muscular torticollis: A 2018 evidence-based clinical practice guideline from the APTA Academy of Pediatric Physical Therapy. *Pediatr. Phys. Ther., 30(4)*:240-90, 2018.

Lehoux, M. C.; Sobczak, S.; Cloutier, F.; Charest, S. & Bertrand-Grenier, A. Shear wave elastography potential to characterize spastic muscles in stroke survivors: Literature review. *Clin. Biomech. (Bristol), 72*:84-93, 2020.

Maneenin, C.; Maneenin, N.; Jirapornkul, C.; Chaimontri, C. & Iamsaard, S. Classification of sternocleidomastoid muscle variations and comparison of its incidence among populations. *Int. J. Morphol., 41(1)*:175-80, 2023.

Qiu, X.; Cui, Z.; Tang, G.; Deng, H.; Xiong, Z.; Han, S. & Tang, S. Effectiveness and safety of botulinum toxin injections for the treatment of congenital muscular torticollis. *J. Craniofac. Surg., 31(8)*:2160-6, 2020.

Sargent, B.; Kaplan, S. L.; Coulter, C. & Baker, C. Congenital muscular torticollis: Bridging the gap between research and clinical practice. *Pediatrics, 144(2)*:e20190582, 2019.

Silawal, S. & Schulze-Tanzil, G. Sternocleidomastoid muscle variations: A mini literature review. *Folia Morphol. (Warsz.), 82(3)*:507-12, 2022.

Wang, D.; Chen, P.; Jia, F.; Wang, M.; Wu, J. & Yang, S. Division of neuromuscular compartments and localization of the center of the highest region of muscle spindle abundance in deep cervical muscles based on Sihler's staining. *Front. Neuroanat., 18*:1340468, 2024.

Wang, J.; Li, Y.; Wang, M. & Yang, S. Localization of the center of the intramuscular nerve dense region of the suboccipital muscles: An anatomical study. *Front. Neurol., 13*:863446, 2022.

Yu, J.; Li, Y.; Yang, L.; Li, Y.; Zhang, S. & Yang, S. The highest region of muscle spindle abundance as the optimal target of botulinum toxin A injection to block muscle spasms in rats. *Front. Neurol., 14*:1061849, 2023.

Zhou, J.; Jia, F.; Chen, P.; Zhou, G.; Wang, M.; Wu, J. & Yang, S. Localisation of the centre of the highest region of muscle spindle abundance of anterior forearm muscles. *J. Anat., 244(5)*:803-14, 2023.

Corresponding author:
Shengbo Yang
Department of Anatomy
Zunyi Medical University
6 University West Road
Xinpu New Developing Areas
Zunyi City
Guizhou Province
Postal code: 563099
CHINA

E-mail: yangshengbo8205486@163.com